



HAL
open science

Dipolar Nanocars Based on a Porphyrin Backbone

Toshio Nishino, Colin Martin, Hiroki Takeuchi, Florence Lim, Kazuma Yasuhara, Yohan Gisbert, Seifallah Abid, Nathalie Saffon-merceron, Claire Kammerer, Gwénaél Rapenne

► **To cite this version:**

Toshio Nishino, Colin Martin, Hiroki Takeuchi, Florence Lim, Kazuma Yasuhara, et al.. Dipolar Nanocars Based on a Porphyrin Backbone. *Chemistry - A European Journal*, 2020, 26 (52), pp.12010-12018. 10.1002/chem.202001999 . hal-03636867

HAL Id: hal-03636867

<https://hal.science/hal-03636867>

Submitted on 13 May 2022

HAL is a multi-disciplinary open access archive for the deposit and dissemination of scientific research documents, whether they are published or not. The documents may come from teaching and research institutions in France or abroad, or from public or private research centers.

L'archive ouverte pluridisciplinaire **HAL**, est destinée au dépôt et à la diffusion de documents scientifiques de niveau recherche, publiés ou non, émanant des établissements d'enseignement et de recherche français ou étrangers, des laboratoires publics ou privés.

Dipolar Nanocars Based on a Porphyrin Backbone

Toshio Nishino,^[a] Colin J. Martin,^[a,b] Hiroki Takeuchi,^[a] Florence Lim,^[a]
Kazuma Yasuhara,^[a] Yohan Gisbert,^[c] Seifallah Abid,^[c]
Nathalie Saffon-Merceron,^[d] Claire Kammerer,^[c] and Gwénaél Rapenne*^[a,b,c]

- [a] Dr. T. Nishino, Dr. C.J. Martin, H. Takeuchi, F. Lim, Dr. K. Yasuhara, Prof. Dr. G. Rapenne
Division of Materials Science, Nara Institute of Science and Technology, 8916-5 Takayama,
Ikoma, Nara 630-0192, Japan
E-mail: gwenaël-rapenne@ms.naist.jp
Homepage: <https://mswebs.naist.jp/LABs/biomimetic/index.html>
- [b] Dr. C.J. Martin, Prof. Dr. G. Rapenne
International Collaborative Laboratory for Supraphotocative Systems, NAIST-CEMES, 29 rue
Marvig, 31055 Toulouse, France
- [c] Y. Gisbert, Dr. S. Abid, Dr. C. Kammerer, Prof. Dr. G. Rapenne
CEMES, Université de Toulouse, CNRS, 29, rue Marvig, 31055 Toulouse, France
- [d] Dr. N. Saffon-Merceron,
Université de Toulouse, UPS, Institut de Chimie de Toulouse,
ICT FR 2599, 118 route de Narbonne, 31062 Toulouse, France

Dedicated to Professor Jean-Marie Lehn on the occasion of his 80th birthday

Abstract

The design and synthesis of a new family of nanocars is reported. To control their motion, we integrated a dipole which can be tuned thanks to strategic donor and acceptor substituents at the 5- and 15-positions of the porphyrin backbone. The two other meso positions are substituted with ethynyltriptycene moieties which are known to act as wheels. Full characterization of nine nanocars is presented as well as the electrochemistry of these push-pull molecules. DFT calculations allowed us to evaluate the magnitude of the dipoles and to understand the electrochemical behavior and how it is affected by the electron donating and accepting groups present. An X-ray crystal structure of one nanocar has also been obtained.

Preprint

Submitted to *Chem. Eur. J.*

INTRODUCTION

Molecular vehicles or nanocars are molecular machines able to be moved in a controlled manner at the nanoscale on a surface. The first prototypes were technomimetic^[1] containing both chassis and four wheels.^[2-4] In this technomimetic family, Feringa et al. proposed a very impressive nanovehicle with four motors as wheels.^[5] Nevertheless, such nanocars were often designed to mimic the function of vehicles without keeping the structural design of macroscopic cars. For instance, recent developments (see below) have shown that the function of vehicles can be maintained at the nanoscale with less and even no wheels. In 2013, in a perspective article named "Molecule concept nanocars: Chassis, wheels and motors?"^[6], a competition was proposed whereby all nanocar designers could meet to test and compare their prototypes. This challenge stimulated the design and the synthesis of many kinds of nanocars following, or not, technomimetic designs, some of which participated in the first nanocar race four years later. This nanocar race was held on a metallic surface inside of a 4-tip STM with an independent control for each tip and allowed for the deposition by sublimation of four molecules with different mass, composition and sublimation temperature. Six competitors from Austria, Germany, Japan, Switzerland, USA and France participated with their own design and strategies to speed up and control the motion of their nanocars on a metallic surface.^[7] The variety of the molecules was very wide with structures containing from 42 atoms ($C_{22}H_{17}N_3$) for the Swiss team^[8] to 642 atoms ($C_{244}H_{222}N_{120}O_{56}$) for the US team.^[9]

Three nanocars, those from the USA, Austria and France, were technomimetic containing general shapes similar to a macroscopic car with a planar chassis and two to four wheels.^[9-11] The other groups from Japan, Germany and Switzerland did not use wheels since mobility at the nanoscale does not require them^[12-14] as nanovehicle designs do not follow the same rules as macroscopic vehicles. For instance, to deal with the gravity forces at the macroscopic level, wheel rotation is very efficient, but at the nanoscale gravity is negligible compared to van der Waals interactions between molecules and the surface. To have an efficient nanocar two criteria are essential: first molecules must be able to diffuse on the surface, so the molecule-surface interaction must be minimized. Second, to be able to control the direction of the motion a good understanding of the mechanism of this motion is needed. For example, the very smart butterfly-shaped nanocar developed by the Japanese team used binaphthyl fragments to separate the molecule from the metallic substrate, but also as a source of motion provided by the inelastic excitation of the molecule without any mechanical contact of the STM tip.^[12] In our case, the molecule we proposed as a nanocar was based on a large polyaromatic hydrocarbon chassis^[15] functionalized with four triptycene wheels (Figure 1).^[16] Despite the advantage of being very robust, our molecule was not mobile without mechanical contact and only direct pushing or pulling with the STM tip was able to induce a motion.^[17]

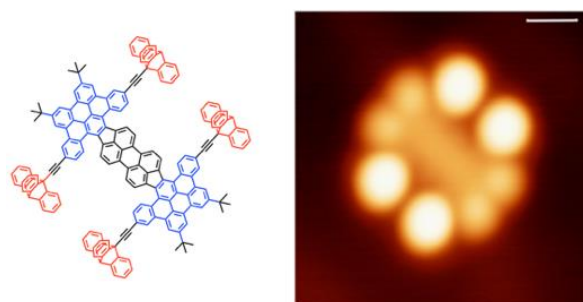


Figure 1. Chemical structure and STM image on Au(111) of the nanocar used in the first nanocar race ($U = 1.1$ V, $I = 5$ pA). Scale bar: 1 nm.

In our research on molecular motors,^[18-19] we synthesized a double-decker motor with a dipolar rotor and have been able to rotate it clockwise or counter-clockwise synchronously as a self-assembled monolayer without any mechanical contact by using the electric field generated by the tip apex of the STM.^[20] James Tour, one of the pioneers in the field of nanocars, was the first to explore the ability of dipoles as effective handles under the effect of an electric field.^[21] This non-contact strategy to control the motion of dipolar molecules at the nanoscale was confirmed during the first nanocar race, where the fastest nanocars were found to also have a strong permanent dipole.^[8,10]

In 2021, a second nanocar race will be organized.^[22] For this new challenge, we decided to exploit movable dipolar molecules. In this article we describe the design and synthesis of a nanocar family with a tunable permanent dipole to explore the influence of the magnitude of the dipole on the properties of the nanocar in term of speed, movability and directionality. For instance, intuitively, we could think that increasing the value of the dipole would increase the speed of the molecule. But is it correct at the nanoscale where intuition often does not follow the quantum laws? Is it still possible to keep control of the molecule?

Herein we report the design and synthesis of a new family of nanocars built on a central porphyrin backbone, a very stable organic architecture which offers the possibility to be functionalized dissymmetrically using many types of substituent groups. DFT calculations and electrochemical analysis have been performed to systematically understand the behavior of such molecules.

RESULTS AND DISCUSSION

Molecular design

Our general design is shown in Figure 2, porphyrins were selected as the central platform because of their planar structure and high stability. They are also rigid molecular structures which is desirable to allow for a minimum number of degrees of freedom and to maximize the direct conversion of electric field-dipole interactions into translational motion. Since preparation of porphyrins is very versatile and can give rise to many types of substitution at the meso position,^[23-24] it is possible to fine tune the amplitude of the dipole moment with minimal change in the synthetic strategy. A combination of pertinent electron-donating and electron-withdrawing substituents can give us access to a family of varying dipoles. This will allow us to manipulate molecules without direct contact with the electric field induced by the STM tip. Another parameter to be minimized by design is the diffusion energy of the molecule.

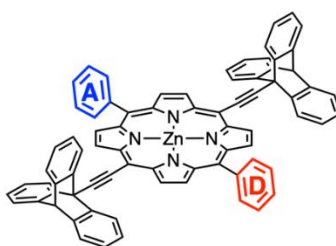


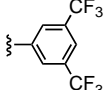
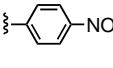
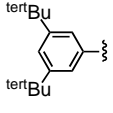
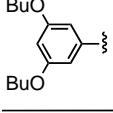
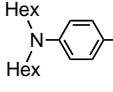
Figure 2. General structure of the nanocars described in this paper. A represents an acceptor (electron-withdrawing functionalized phenyl group) and D is a donor (electron-donating functionalized phenyl group).

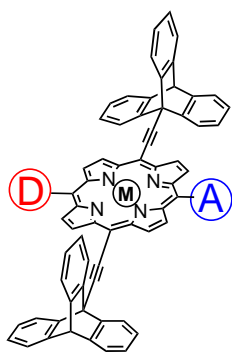
Large and rigid polyaromatic π -molecules tend to interact strongly with the metallic surface, limiting the movability of the molecule.^[25] To enhance this, the aromatic planar structure of the porphyrin has to be lifted up from the surface. For that purpose, donor and acceptor substituents have been introduced on the phenyl ring at the 5- and 15-positions. These phenyl groups can't be coplanar with the porphyrin backbone which contribute to the lift up of the porphyrin as well as the presence of triptycenes introduced at the two other meso positions (10 and 20). These fragments are also known to diffuse easily on the surface and have sometimes been shown to have the capacity to rotate.^[26] A lower diffusion energy will result in a better movability by decreasing the physical and/or chemical adsorption of the molecule onto the surface. The porphyrin has to be metallated to avoid partial metalation on the metallic surfaces used. In addition, it is well-known that porphyrins can form supramolecular architectures *via* axial coordination to a metal center as in the case of zinc,^[27] or by π - π interactions, implying that our designed nanocars have potential applications in loading and carrying cargo molecules.

Determination of the dipole moment by DFT calculation

DFT calculations of metal-free and zinc containing porphyrin-based nanocars were carried out to systematically investigate the influence of substituents introduced onto the porphyrin ring on the molecules' dipole moment. All calculations were performed with the Gaussian09 suite of programs^[28] in vacuo, using the WB97XD functional, taking into account long range interactions and dispersion corrections with the 6-31G* basis set, a larger basis set than the 6-21G* reported for previous similar compounds^[29]. We selected three kinds of electron-donating groups, namely 3,5-bis-*tert*-butylphenyl, 3,5-dibutoxyphenyl and 4-*N,N*-dihexylaminophenyl, and three kinds of electron-withdrawing units, namely 3,5-bis-trifluoromethylphenyl, 4-cyanophenyl and 4-nitrophenyl. The results of DFT dipole calculations are summarized in table 1.

Table 1. DFT calculations of the dipole moment of the free-base porphyrins and their zinc containing analogues.

				
	M = H ₂ : 6.9 D M = Zn : 6.9 D [1d]	5.1 D 5.0 D [2d]	7.1 D 7.1 D [3d]	
	M = H ₂ : 9.7 D M = Zn : 9.7 D [4d]	7.8 D 7.8 D [5d]	9.9 D 9.9 D [6d]	
	M = H ₂ : 9.3 D M = Zn : 9.2 D [7d]	7.7 D 7.6 D [8d]	9.5 D 9.4 D [9d]	

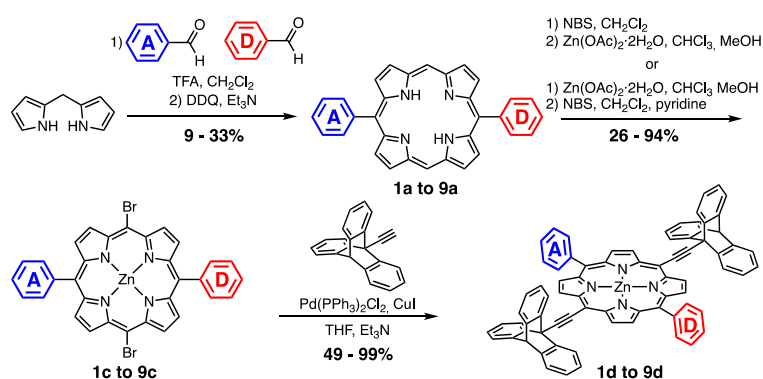


The dipole moments range from 5.0 D to 9.9 D. As expected, the presence of the zinc metal center has negligible influence on the dipole, with a calculated slightly lower value of about 0.1 D in each case.

The smallest dipole moment (5.0 D) was estimated for the nanocar having 3,5-bis-*tert*-butylphenyl and 3,5-bis-trifluoromethylphenyl as electron-donating and electron-withdrawing groups, respectively (**2d**). On the other hand, the largest dipole moment (9.9 D) was observed for the nanocar having 3,5-dibutoxyphenyl and 4-nitrophenyl groups (**6d**). This result implied that our methodology, namely introduction of electron-donating and -withdrawing group as a perturbation module unit, enables us to control the total dipole moment precisely with a wide variety of amplitude.

Synthesis

The general synthetic scheme for porphyrin-based nanocars **1d** to **9d** is detailed in Scheme 1. Porphyrins having different substituents at the 5- and 15-positions, which are key structures of our nanocars were synthesized by conventional methods, namely condensation of two different aldehydes and dipyrromethane followed by oxidation of the intermediate porphyrinogen.^[30] The symmetric porphyrins and polymeric species were removed by silica gel column chromatography and reprecipitation to afford the desired dissymmetric porphyrins **1a** to **9a** in moderate yields. Porphyrins having 3,5-di-*tert*-butylphenyl or 3,5-dibutoxyphenyl units as electron-donating groups were converted into their zinc complexes. The meso positions of these zinc porphyrins were then brominated using *N*-bromosuccinimide to obtain the nanocar precursors **1c** to **6c**.



Scheme 1. General synthetic scheme of dipolar porphyrin-based nanocars **1d** to **9d**.

In the case of porphyrins having 4-*N,N*-dihexylaminophenyl groups, bromination *via* the same scheme did not work well due to the occurrence of further brominations on the 4-di-hexylaminophenyl moiety. This over-bromination is certainly due to the strong electron donating character of the dialkylamino moiety on the phenyl ring. Instead we carried out bromination of the free-base porphyrins **7a** to **9a** at -40°C followed by zinc complexation to give **7c** to **9c** in satisfying yield. 9-Ethynyltriptycene^[31] was introduced on the brominated meso positions of the porphyrin scaffold using Sonogashira coupling conditions to afford the porphyrin-based nanocars **1d** to **9d** as their zinc complexes.

The nine porphyrin-based nanocars (Table 1) have been synthesized following this general strategy. These have been fully characterized by $^1\text{H-NMR}$, $^{13}\text{C-NMR}$, 2D NMR, UV-Visible spectroscopy, MALDI-TOF MS, electrochemistry, and one of them by single crystal X-ray analysis. All the data are given in the experimental part and supporting information.

As a representative example we will discuss in more detail the characterization of the nanocar with 3,5-di-*tert*-butylphenyl as the donor and 4-cyanophenyl as the acceptor group (**1d**). UV-visible spectroscopy

showed the expected characteristic porphyrin absorptions, with an intense Soret band at 438 nm and a pair of Q bands at 580 and 629 nm. MALDI-TOF MS gave the molecular ion peak $[M]^+$ corresponding to the nanocar at $m/z = 1213.5$ which is in agreement with the calculated isotopic pattern (Figure S19a of the supporting information). All the nanocars synthesized showed similar behaviors (Table 2 and Figure S22 of the supporting information). We can notice that nanocars containing the 4-*N,N*-dihexylaminophenyl donating group (**7d**, **8d** and **9d**) show a relative decrease in their molar extinction coefficient but the bands are strongly enlarged, maybe because of some H-bonds between the amino group and the solvent. After excitation in the Soret band, the nanocars emit light in the red color from 632 to 635 nm for **1d** to **6d** and at lower energies (646 to 652 nm) for nanocars **7d** to **9d**. Additionally, apolar symmetric analogues carrying two donors such as 3,5-bis-*tert*-butylphenyl (**10d**), 3,5-dibutoxyphenyl (**11d**) and 4-*N,N*-dihexylaminophenyl groups (**12d**) were studied in comparison with their polar counterparts.

Table 2. UV-Visible data (full spectra given in SI) and luminescence properties of the nanocars **1d** to **9d** and their apolar symmetric analogues **10d** to **12d**. ($[Substrate] = 2 \mu M$ in $CHCl_3$)

N°	λ_{max} (ε) Soret		λ_{max} (ε) Q-bands		Luminescence	
	nm ($mol^{-1}dm^3cm^{-1}$)				Exc. (nm)	Em. (nm)
1d	438 (493600)	580 (17200)	629 (40300)		438	635
2d	438 (522900)	581 (17300)	629 (40950)		438	634
3d	439 (396850)	580 (18050)	630 (48800)		438	634
10d	437 (495600)	580 (14800)	632 (41200)		438	637
4d	439 (483300)	581 (17600)	628 (37000)		439	633
5d	439 (526550)	579 (17400)	627 (37500)		439	632
6d	439 (404900)	580 (18500)	627 (37250)		439	632
11d	439 (538950)	580 (16350)	629 (38800)		439	634
7d	435 (268250)	584 (13750)	635 (27800)		435	651
8d	435 (275850)	584 (13850)	635 (27200)		435	652
9d	436 (231250)	585 (14300)	635 (27550)		435	646
12d	432 (165300)	587 (12050)	642 (28200)		435	661

The aromatic region of the 1H -NMR spectrum (Figure 3) fits very well with the expected structure of **1d** and indicates that this nanocar has C_s symmetry in solution. Four sets of doublets corresponding to the protons at the β -pyrrolic positions of the porphyrin are observed (solid circle, Figure 3), confirming the 5,15-dissymmetrically-substituted structure. Moreover, observation of four sets of triptycene signals (solid triangle, Figure 3) implied that structural oscillation of the two triptycenes around the ethynyl spacer is fast enough on NMR timescales. Comparison of integrals of the triptycenylic signals with the porphyrin's protons confirms a ratio of two triptycenes per porphyrin.

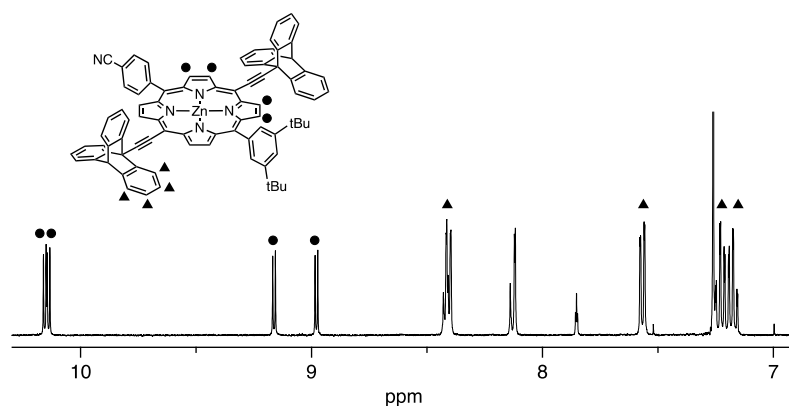


Figure 3. Aromatic region of the $^1\text{H-NMR}$ spectrum of the nanocar **1d** with a 3,5-di-*tert*-butylphenyl as donor group and 4-cyanophenyl as accepting group (400 MHz, CDCl_3). Protons corresponding to β -positions of porphyrin ring and to triptycenes were depicted as solid circle (●) and solid triangle (▲), respectively.

X-ray structure

Single crystals of the nanocar **1d** with 3,5-di-*tert*-butylphenyl as donor group and 4-cyanophenyl as acceptor group (Figure 3) that were suitable for X-ray structural analysis were obtained by diffusion of methanol vapor into a benzene solution containing the nanocar. As shown in Figure 4, neighboring porphyrins arranged in an antiparallel fashion to annihilate the total dipole moment of the crystal. Compared to the DFT calculated structure, the molecule in the crystal is slightly bent due to some intermolecular CH- π interactions not present in the calculations. Furthermore, a methanol molecule, used as non-solvent to crystallize the molecule, coordinates at the axial position of the zinc ion in a classical manner.^[32] As a result the zinc ion shows a square pyramidal coordination geometry and is located slightly out of the plane defined by the four pyrrolic nitrogens of the porphyrin ($d=0.270(2)$ Å). This shows the ability of this porphyrin-based nanocar to load cargo molecules through axial coordination to the zinc center.

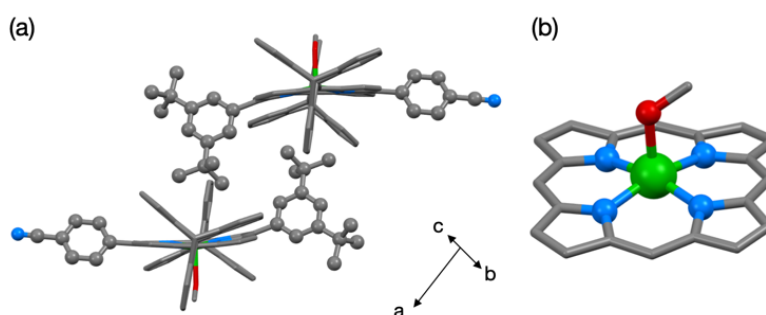


Figure 4. Side view (a) of the molecular structure of two neighboring nanocars **1d** showing their antiparallel arrangement and the coordination geometry of porphyrin center (b, meso substituents were omitted in this view). The hydrogen atoms and crystal solvents were omitted for clarity. Color code: Zn, green; C, gray; N, blue; O, red.

Electrochemical properties of the nanocars

The effect of the electron-donating and electron-withdrawing substituents introduced into the porphyrin backbone on the redox properties was examined using cyclic voltammetry in dichloromethane. Figure 5 shows the voltammograms of the porphyrin-based nanocar series containing 3,5-di-*tert*-butylphenyls as electron donating units (**1d** to **3d**) along with their symmetrically substituted analogue **10d**. Upon oxidation all four compounds gave rise to two reversible redox waves (Figure 5) which can be attributed to the one electron oxidation of the porphyrin ring ($E_0' = 0.51$ V and 0.84 V for **2d**, 0.49 V and 0.82 V for **1d**, 0.49 V and 0.82 V for **3d** vs. Fc/Fc⁺). Comparing with the symmetrically substituted porphyrin with two 3,5-di-*tert*-butylphenyl groups **10d** ($E_0' = 0.42$ V and 0.77 V vs. Fc/Fc⁺), a positive shift in oxidation potentials (approximately 50 to 90 mV) was observed resulting from the increasing electron density in the HOMO, related to the donating groups present. This behavior appears reasonable taking into account the results of the DFT calculations as the electron density of the HOMO orbital is localized onto the central porphyrin ring rather than peripheral phenyl ring (see SI figures S31 and S32).

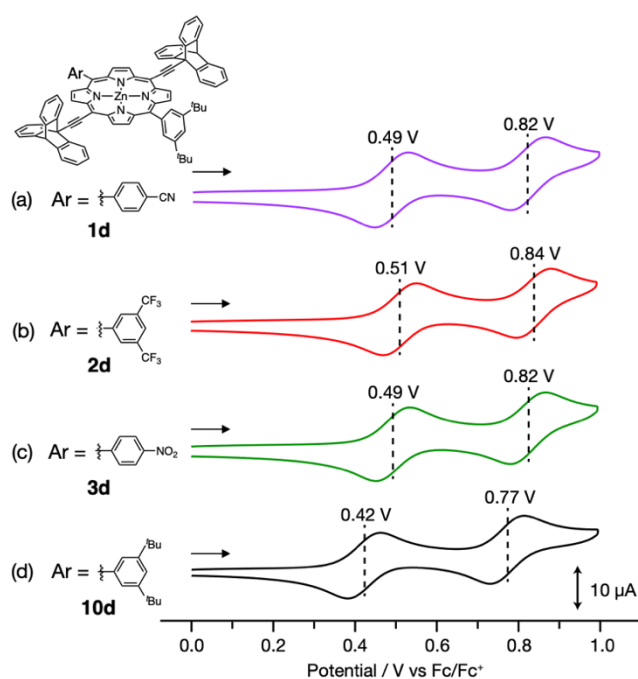


Figure 5. Cyclic voltammograms of oxidation region of Zn porphyrin derivatives **1d-3d** and **10d** having a 3,5-di-*tert*-butylphenyl substituent on the 5-position and a 4-cyanophenyl (a), 3,5-bis(trifluoromethyl)phenyl (b), 4-nitrophenyl (c) or 3,5-di-*tert*-butylphenyl (d) substituent on the 15-position, in CH₂Cl₂ containing 0.1 M TBAPF₆ at 20 °C at a scan rate of 100 mV.s⁻¹. [Substrate] = 500 μM.

Similar patterns are observed (See Supporting information) for the nanocars having 3,5-dibutoxyphenyl moieties as the electron donating groups (**4d** to **6d**), with oxidations seen between $E_0' = 0.49$ -0.50 V and 0.82-0.84 V, in each case (Figure S25 in the Supporting Information). Here again the oxidation potentials are at slightly higher compared to their symmetrically substituted analogue **11d** which occur at $E_0' = 0.46$ V and 0.78 V. Interestingly all of the porphyrins containing the 4-*N,N*-dihexylaminophenyl donating group (**7d** to **9d**) show a relative decrease in oxidation potential at 0.33 V and between 0.51-0.52 V, while the symmetrically substituted 4-*N,N*-dihexylaminophenyl analogue porphyrin **12d** shows

a further decrease to as low as 0.24 V and 0.36 V. This can be rationalized from the DFT calculations of the porphyrins in which contribution to the HOMO from the electron donating groups is only observed for the 4-*N,N*-dihexylaminophenyl compounds (see SI). As such it would be predicted that these are the only cases in which the substituent affects the HOMO stability and the resulting electrochemical oxidation potential.

Looking at the electrochemical reductions, a number of trends can also be observed. In most cases application of a negative potential results in low current irreversible reductions starting below -1.45 V. This is observed for all systems except one, indicating these irreversible reductions occur on the peripheral groups rather than the porphyrin core; as the symmetric analogue of the 3,5-di-*tert*-butylphenyl porphyrins **10d** is the only case where such reductions cannot occur it is the only system where they are not observed (Figure 6). This is followed by a single electron quasi-reversible reduction (of similar current response to the one electron oxidations) between -1.58 V and -1.81 V (Figure 6 and Table 3, mentioned as Red₂). As with the oxidations these reductions vary with the electronic nature of the substituents present; however it is the electron-withdrawing group that affects the reduction potential rather than the electron-donating group as in the oxidation cases. With the 4-nitrophenyl withdrawing group having the largest effect, either positive or negative, on the reduction potential. That the electron-donating part of the molecule affects the oxidation potential (and HOMO level) while the electron-withdrawing part affects the reduction potential (and LUMO level) offers an excellent method for the tuning of future targets both in terms of electronic properties and dipole moments

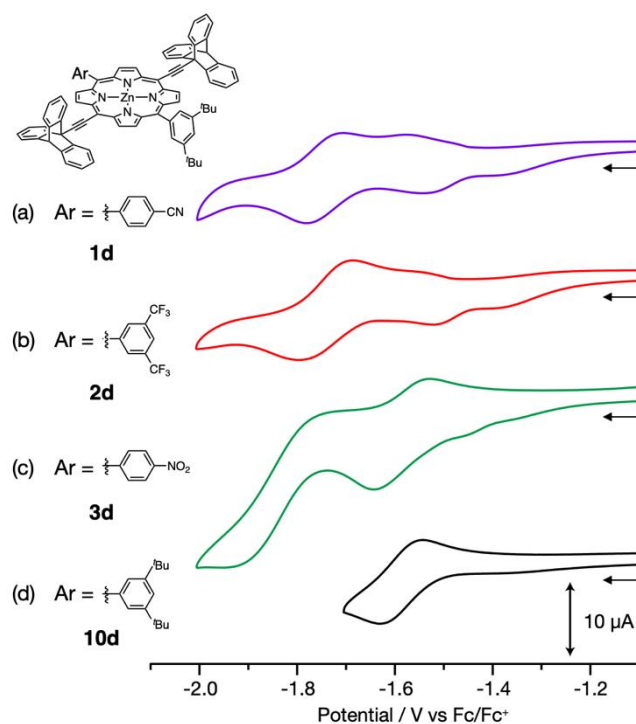


Figure 6. Cyclic voltammograms of reduction region of Zn porphyrin derivatives **1d-3d** and **10d** having a 3,5-di-*tert*-butylphenyl substituent on the 5-position and a 4-cyanophenyl (a), 3,5-bis(trifluoromethyl)phenyl (b), 4-nitrophenyl (c) or 3,5-di-*tert*-butylphenyl (d) substituent on the 15-position, in CH_2Cl_2 containing 0.1 M TBAPF₆ at 20 °C at a scan rate of 100 $\text{mV}\cdot\text{s}^{-1}$. [Substrate] = 500 μM .

Using these reversible electrochemical oxidations and quasi-reversible reductions, an estimation of the frontier orbital levels for each zinc porphyrin complex can be calculated from the onset potential of each redox response^[33]. This gives values of the band gap for each complex that can be compared to both those calculated from the onset of the Soret band in the absorption spectra and for the calculated orbitals of the zinc porphyrins by DFT. It is important to note that due to the presence of solvent and electrolyte, it is not reasonable to compare the band gap values obtained directly with those calculated using DFT or absorption. However a systematic comparison of the trends resulting from changes in donors and acceptors will give information on their effect and how they are seen from different methods. Such a comparison shows clear trends in the band gaps with the smallest values always observed in the presence of 4-*N,N*-dihexylaminophenyl electron donating groups and those systems containing 4-nitrophenyl electron withdrawing groups deviating the most from the others.

Table 3. Electrochemical redox potentials (in V vs Fc/Fc⁺), and band gaps (in eV) from electrochemical data, UV-Vis spectra and DFT calculations for all zinc nanocars **1d** to **9d** with the corresponding aromatic groups Ar₁ and Ar₂ and their apolar symmetric analogues **10d** to **12d**.

Ar ₁	Ar ₂	N ^o	Red ₂ ^a	Red ₁	Red _{on}	Ox ₁	Ox ₂	Ox _{on}	Band gap (eV)		
									From CV ^b	From DFT ^c	From UV-Vis ^d
-(3,5-di ^t Bu)Ph]	-[(4-CN)Ph]	1d	-1.77	-1.54 ⁱ	-1.58	0.49	0.82	0.41	1.99	5.28	2.66
-(3,5-di ^t Bu)Ph]	-[(3,5-diCF ₃)Ph]	2d	-1.80	-1.52 ⁱ	-1.56	0.51	0.84	0.44	2.00	5.27	2.67
-(3,5-di ^t Bu)Ph]	-[(4-NO ₂)Ph]	3d	-1.60	-1.60 ⁱ	-1.45	0.49	0.82	0.42	1.87	5.28	2.60
-(3,5-di ^t Bu)Ph]	-[(3,5-di ^t Bu)Ph]	10d	-1.58	-	-1.50	0.42	0.77	0.35	1.85	5.25	2.66
-(3,5-di ^t OBu)Ph]	-[(4-CN)Ph]	4d	-1.72	-1.54 ⁱ	-1.58	0.49	0.82	0.42	2.00	5.30	2.64
-(3,5-di ^t OBu)Ph]	-[(3,5-diCF ₃)Ph]	5d	-1.70	-1.52 ⁱ	-1.55	0.50	0.84	0.43	1.98	5.30	2.66
-(3,5-di ^t OBu)Ph]	-[(4-NO ₂)Ph]	6d	-1.80	-1.61 ⁱ	-1.68	0.50	0.83	0.43	2.11	5.29	2.57
-(3,5-di ^t OBu)Ph]	-[(3,5-di ^t OBu)Ph]	11d	-1.81	-1.61 ⁱ	-1.62	0.46	0.78	0.39	2.01	5.29	2.67
-[4-N(Hex) ₂ Ph]	-[(4-CN)Ph]	7d	-1.81	-1.54 ⁱ	-1.57	0.33	0.51	0.25	1.82	5.20	2.42
-[4-N(Hex) ₂ Ph]	-[(3,5-diCF ₃)Ph]	8d	-1.78	-1.42 ⁱ	-1.59	0.33	0.52	0.25	1.84	5.18	2.42
-[4-N(Hex) ₂ Ph]	-[(4-NO ₂)Ph]	9d	-1.68	-1.56 ⁱ	-1.54	0.33	0.52	0.25	1.79	5.21	2.40
-[4-N(Hex) ₂ Ph]	-[4-N(Hex) ₂ Ph]	12d	-1.77	-1.62 ⁱ	-1.60	0.24	0.36	0.17	1.77	5.16	2.40

^a Red₂ are all quasi-reversible

^b Determined from electrochemical values of the HOMO and LUMO (Ox_{on} - Red_{on}) for the Zn porphyrins

^c Calculated from DFT values of the HOMO and LUMO for the Zn porphyrins in the gas phase

^d Determined from the onset potential of the Soret band in the UV-Vis. spectra for the Zn porphyrins

ⁱ = irreversible reduction (ignored for onset).

CONCLUSIONS

In this work, a series of nine prototypes of dipolar nanocars with different amplitude of dipole moments from 5.0 to 9.9 D were prepared and fully characterized. One of these nanocars (**1d**) is also already registered to participate in the second nanocar race which will be organized in 2021.^[22]

Work is now underway to investigate by STM the correlation between the amplitude of the dipole moment of the nanocar with their movability on metallic surfaces. We would like to establish the laws describing the motion of such molecules at the nanoscale under the influence of an STM tip-induced electric field. The more efficient nanocar will be the one with the best compromise between the speed and the controllability.

Such donor-acceptor porphyrins may also find applications in thin film devices and materials including light emitting devices, photovoltaic cells and field effect transistors.^[34-36]

EXPERIMENTAL SECTION

A typical synthetic procedure is described below for the nanocar with a 3,5-di-*tert*-butylphenyl as donor group and 4-cyanophenyl as accepting group (**1d**). All the other nanocars presented in Table 1 (**2d to 9d**) are described in the supporting information document. The apolar nanocars with trans-A₂B₂ porphyrins, used as reference in the electrochemistry section, have been synthesized following the same synthetic strategy from the following porphyrins. 5,15-(3,5-Di-*tert*-butylphenyl) porphyrin **10d** and 5,15-(3,5-dibutoxyphenyl)porphyrin **11d** were synthesized directly *via* condensation of the corresponding aldehydes and dipyrromethane. 5,15-(4-*N,N*-dihexylaminophenyl) porphyrin **12d** was afforded as a byproduct of dissymmetric porphyrin synthesis.

General methods:

Synthetic procedures were carried out under dry nitrogen atmosphere, unless otherwise specified. All reagents and solvents were purchased at the highest commercial quality available and used without further purification, unless otherwise stated. Trifluoroacetic acid, chloroform, 4-nitrobenzaldehyde, copper iodide, methanol, anhydrous *N,N*-dimethylformamide, *N*-bromosuccinimide, and zinc acetate dihydrate were purchased from FUJIFILM Wako Pure Chemical Corporation. 3,5-Bis(*tert*-butyl)benzaldehyde was purchased from Aldrich. Dichloromethane, 2,3-dichloro-5,6-dicyano-1,4-benzoquinone (DDQ), anhydrous tetrahydrofuran and triethylamine were purchased from Nacalaitesque. Pyrrole, 4-cyano-benzaldehyde and bis(triphenylphosphine) palladium(II)dichloride were purchased from TCI. 9-Ethynyltritycene,^[31] dipyrromethane,^[37] 4-(*N,N*-dihexylamino)benzaldehyde^[38] and 3,5-dibutoxybenzaldehyde^[39] were prepared according to the literature procedures. The complexation reaction of a porphyrin with zinc ion under microwave irradiation was carried out by utilizing CEM Discover SP in a glass pressure tube equipped with PTFE-coated magnetic stirring bar. Silica gel column chromatography and thin-layer (TLC) chromatography were performed using Wakosil® 60 and Merck silica gel 60 (F254) TLC plates, respectively. ¹H and ¹³C NMR spectra were recorded on a JEOL JNM-ECA600 (600 MHz for ¹H; 150 MHz for ¹³C) spectrometer or a JEOL JNM-ECX400P (400 MHz for ¹H; 100 MHz for ¹³C) spectrometer at a constant temperature of 298 K. Tetramethylsilane (TMS) was used as an internal reference for ¹H and ¹³C NMR measurements in CDCl₃ and DMSO-*d*₆. Chemical shifts (δ) are reported in ppm. Coupling constants (*J*) are given in Hz and the following abbreviations have been used to describe the signals: singlet (s); broad singlet (br. s); doublet (d); triplet (t); quadruplet (q); quintuplet (quint); multiplet (m). Full assignments of ¹H and ¹³C NMR spectra were made with the assistance of COSY, HMBC, and HSQC spectra when necessary. The MALDI-TOF mass spectrometry was performed using Bruker Daltonics Autoflex II spectrometer and JEOL JMS-S300 spectrometer. DCI mass spectrometry was performed with a Waters GCT Premier spectrometer for desorption chemical ionization (CH₄). The fluorescence spectra were recorded with a Hitachi F-7000 spectrometer in chloroform solution at 20 ± 0.1 °C in 1.0 cm quartz cells. The absorption spectra were obtained using Hitachi U-3310 spectrometer in CHCl₃ solution at 20 ± 0.1 °C in 1.0 cm quartz cells. Absorption Gap values E_{gap} were calculated from the low energy onset frequency of the absorption Soret band (λ_{on}) such that $E_{\text{gap}} = hc/\lambda_{\text{on}}$ giving E_{gap} (in eV) = 1240/ λ_{on} (in nm). Cyclic voltammetry measurements were performed with ALS electrochemical analyzer Model 630DA at room temperature in HPLC grade dichloromethane containing 0.1 M TBAPF₆ as supporting electrolyte at concentrations of 500 μmol in a standard one-component cell, working under an Ar atmosphere and equipped with a ϕ 3 mm glassy carbon working electrode, a Pt wire counter electrode and Ag/Ag⁺ reference electrode at a scan rate of 100 mV.s⁻¹ at 20 °C. All solutions were deoxygenated by Ar bubbling for at least 20 min; the obtained E⁰ vs. Ag/Ag⁺ values were converted into those of Fc/Fc⁺

based on the measured redox potential of ferrocene. TBAPF₆ used as electrolyte was recrystallized from ethanol and dried under reduced pressure for 12 hr at 100 °C. Ferrocene was sublimated under reduced pressure at 80 °C.

5-(3,5-di-*tert*-butylphenyl)-15-(4-cyanophenyl)porphyrin (1a)

This reaction was performed under a nitrogen atmosphere and all reaction vessels were dried up. 3,5-Di-*tert*-butylbenzaldehyde (326 mg, 1.5 mmol), 4-cyanobenzaldehyde (197 mg, 1.5 mmol) and dipyrromethane (440 mg, 3.0 mmol) were dissolved in dichloromethane (300 mL) and the solution was deoxygenated by bubbling nitrogen for 20 min. Trifluoroacetic acid (413 μ L, 5.4 mmol) was added and the resulting solution was stirred at room temperature for 30 min under dark. Then, DDQ (1.0 g, 4.6 mmol) and triethylamine (730 μ L, 6.0 mmol) were added. The reaction mixture was stirred at room temperature for further 2 h, and then silica gel (40 mL) was added. The resulting mixture was evaporated and the crude compound was preadsorbed on the silica gel. The crude material was purified by silica gel column chromatography (5 ϕ x 12 cm, hexane : dichloromethane = 3 : 7) to afford crude purple solid. Washing with acetone gave the free-base porphyrin **1a** as a purple solid (292 mg, 32%). ¹H NMR (600 MHz, CDCl₃/TMS): δ = 10.35 (s, 2H), 9.44 (d, *J* = 4.8 Hz, 2H), 9.42 (d, *J* = 4.8 Hz, 2H), 9.16 (d, *J* = 4.2 Hz, 2H), 8.98 (d, *J* = 4.2 Hz, 2H), 8.42 (d, *J* = 8.4 Hz, 2H), 8.13–8.12 (m, 4H), 7.85 (t, *J* = 1.8 Hz, 1H), 1.57 (s, 18H), -3.09 (d, *J* = 10.8 Hz, 2H); ¹³C NMR (100 MHz, CDCl₃/TMS): δ = 149.2, 147.9, 146.4, 145.5, 145.3, 142.8, 139.7, 134.2, 132.6, 131.8, 131.4, 130.7, 130.5, 130.1, 126.3, 124.2, 122.5, 121.7, 121.5, 121.3, 114.2, 105.7, 35.1, 31.8. HR-MS (DCI/CH₄) calcd. for C₄₁H₃₈N₅ [MH]⁺: 600.3127, found 600.3131.

5-(3,5-di-*tert*-butylphenyl)-15-(4-cyanophenyl)porphyrinato zinc (1b)

A mixture of chloroform (7.5 mL) and methanol (7.5 mL) containing 5-(3,5-di-*tert*-butylphenyl)-15-(4-cyanophenyl)porphyrin (**1a**, 241 mg, 402 μ mol) and Zn(OAc)₂·2H₂O (179 mg, 817 μ mol) was added to the pressure tube. The resulting mixture was heated under microwave irradiation at 100 °C for 20 min, then 120 °C for 3 x 10 min. The reaction mixture was evaporated and the residue was washed with methanol to afford a mixture of the desired compound and the starting free-base porphyrin. The crude material and Zn(OAc)₂·2H₂O (177 mg, 805 μ mol) were heated under microwave irradiation in a mixture of chloroform (10 mL) and methanol (10 mL) at 120 °C for 10 min. After completion of the reaction, the volatiles were evaporated and the residue was washed with methanol and water to afford the zinc porphyrin **1b** as a purple solid (253 mg, 95%). ¹H NMR (400 MHz, DMSO-*d*₆/TMS): δ = 10.40 (s, 2H), 9.55 (d, *J* = 4.4 Hz, 2H), 9.52 (d, *J* = 4.4 Hz, 2H), 8.99 (d, *J* = 4.4 Hz, 2H), 8.92 (d, *J* = 4.4 Hz, 2H), 8.44 (d, *J* = 8.4 Hz, 2H), 8.32 (d, *J* = 7.6 Hz, 2H), 8.08 (s, 2H), 7.87 (s, 1H), 1.56 (s, 18H); ¹³C NMR (100 MHz, DMSO-*d*₆/TMS): δ = 150.2, 149.7, 149.7, 149.4, 148.5, 147.5, 142.0, 135.7, 132.7, 132.2, 131.8, 131.3, 130.1, 124.4, 122.1, 121.5, 120.7, 106.2, 105.7, 35.1, 31.7. HR-MS (ESI): calcd. for C₄₁H₃₅N₅Zn [M]⁺: 661.2184, found 661.2181.

10,20-dibromo-5-(3,5-di-*tert*-butylphenyl)-15-(4-cyanophenyl) porphyrinato zinc (1c)

5-(3,5-di-*tert*-butylphenyl)-15-(4-cyanophenyl)porphyrinato zinc (**1b**, 199 mg, 200 μ mol) was dissolved in a mixture of dichloromethane (55.8 mL) and pyridine (1.2 mL). The solution was stirred in an ice bath. *N*-bromosuccinimide (112 mg, 628 μ mol) was then added to the mixture and the resulting solution was allowed to warm to room temperature. After 20 h of stirring, acetone (20 mL) was added to quench the reaction. The volatiles were evaporated and the residue was washed with methanol to afford the dibrominated porphyrin **1c** as a purple solid (172 mg, 70%). ¹H NMR (400 MHz, DMSO-*d*₆/TMS): δ = 9.67–9.65 (m, 4H), 8.84 (d, *J* = 4.8 Hz, 2H), 8.78 (d, *J* = 4.8 Hz, 2H), 8.37 (d, *J* = 8.0 Hz, 2H), 8.30 (d, *J* = 8.0 Hz, 2H), 7.99 (d, *J* = 1.2 Hz, 2H), 7.88 (t, *J* = 1.6 Hz, 1H), 1.54 (s, 18H); ¹³C NMR

(100 MHz, DMSO-*d*₆/TMS): δ = 156.7, 148.6, 148.4, 148.2, 148.0, 145.3, 144.2, 133.3, 132.7, 132.1, 131.7, 130.8, 128.4, 128.6, 124.5, 122.7, 119.4, 114.6, 114.2, 106.4, 100.2, 67.4, 35.0, 31.7. HR-MS (ESI): calcd. for C₄₁H₃₃Br₂N₅Zn [M]⁺: 817.0394, found 817.0387.

Nanocar 10,20-di(triptycen-9-ylethynyl)-5-(3,5-di-*tert*-butylphe-nyl)-15-(4-cyanophenyl) porphyrinato zinc (1d)

10,20-Dibromo-5-(3,5-di-*tert*-butylphenyl)-15-(4-cyanophenyl)porphyrinato zinc (**1c**, 84 mg, 150 μ mol), 9-ethynyltriptycene (169 mg, 607 μ mol), Pd(PPh₃)₂Cl₂ (11 mg, 16 μ mol) and CuI (3.0 mg, 16 μ mol) were suspended in a mixture of tetrahydrofuran and triethylamine (4 : 1 (v/v), 7.5 mL). The resulting mixture was deoxygenated by freeze-pump-thaw method (three times) and then refluxed for 12 h. The reaction mixture was filtered through celite and the filtrate evaporated. The crude compound was preadsorbed onto silica gel (5 mL) and purified by silica gel column chromatography (4 ϕ x 14 cm, hexane : dichloromethane = 4 : 6) to afford a crude green solid. This solid was further purified by reprecipitation from dichloromethane and methanol to give the nanocar **1d** as a green solid (123 mg, 67%). ¹H NMR (400 MHz, CDCl₃/TMS): δ = 10.16 (d, *J* = 4.8 Hz, 2H), 10.14 (d, *J* = 4.8 Hz, 2H), 9.16 (d, *J* = 5.2 Hz, 2H), 8.98 (d, *J* = 4.8 Hz, 2H), 8.43–8.40 (m, 8H), 8.13–8.11 (m, 4H), 7.85 (t, *J* = 1.8 Hz, 1H), 7.57 (dd, *J* = 1.0, 7.5 Hz, 6H), 7.23 (td, *J* = 1.2, 7.5 Hz, 6H), 7.17 (td, *J* = 1.3, 7.4 Hz, 6H), 5.64 (s, 2H), 1.57 (s, 18H). ¹³C NMR (150 MHz, CDCl₃/TMS): δ = 152.7, 152.5, 151.0, 149.4, 148.9, 147.2, 145.1, 144.7, 140.8, 134.8, 134.2, 132.5, 132.0, 131.6, 130.6, 129.6, 126.0, 125.6, 123.8, 122.9, 121.4, 119.9, 111.9, 101.7, 94.7, 91.8, 54.9, 53.5, 35.1, 31.8; HR-MS (MALDI, DCTB): calcd. for C₈₅H₅₉N₅Zn [M]⁺: 1213.4062, found 1213.4053; UV/Vis (CHCl₃): λ_{\max} (ϵ / mol⁻¹dm³cm⁻¹) = 438 (489100), 580 (17200), 629 nm (40300).

Crystal data of nanocar with a 3,5-di-*tert*-butylphenyl as donor group and 4-cyanophenyl as accepting group (1d):

Single crystals grown in a mixture of benzene/methanol were selected in mother liquor from a flask and covered with perfluorated polyether oil on a microscope slide. An appropriate crystal was selected using a polarizing microscope, fixed on the tip of a MiTeGen© MicroMount, transferred to a goniometer head, and shock cooled by the crystalcooling device. Crystallographic data for the nanocar were collected at 193(2) K on a Bruker-AXS Kappa APEX II Quazar diffractometer equipped with a 30W air-cooled microfocus source using Mo K α radiation (λ =0.71073 Å). Phi- and omega-scans were used. Space group was determined on the basis of systematic absences and intensity statistics. Semi-empirical absorption correction was employed.^[40] The structure was solved using an intrinsic phasing method (SHELXT),^[41] and refined using the least-squares method on F^2 .^[41] All non-H atoms were refined with anisotropic displacement parameters. Hydrogen atoms were refined isotropically at calculated positions using a riding model with their isotropic displacement parameters constrained to be equal to 1.5 times the equivalent isotropic displacement parameters of their pivot atoms for terminal sp³ carbon and 1.2 times for all other carbon atoms. The selected crystal was very weakly diffracting and it was not possible to model the disorder of 1.5 molecules of solvent (C₆H₆). Therefore, the SQUEEZE^[42] function of PLATON was employed to remove this residual electron density. CCDC-1997293 contains the supplementary crystallographic data for this paper. These data can be obtained free of charge from The Cambridge Crystallographic Data Centre via <https://www.ccdc.cam.ac.uk/structures/>. Selected data: C₈₆H₆₂N₅OZn, C₆H₆, *M*=1324.88, monoclinic, space group *C2/c* *a*=46.699(10) Å, *b*= 30.016(6) Å, *c*=11.760(2) Å, α =90°, β =99.082(5)°, γ =90° *V*=16278(6) Å³, *Z*=8, crystal size 0.300 x 0.030 x 0.020 mm³, 219187 reflections collected (14328 independent, *R*_{int} = 0.3675), 899 parameters, 0 restraints, *R*₁[*I*>2 σ (*I*)]=0.0909, *wR*₂[all data]=0.2829, largest diff. peak and hole: 0.447 and -0.579 eÅ⁻³. More details can be found in the Supporting Information.

Computational Methods:

All calculations were performed with the Gaussian09 package.^[28] We used the hybrid dispersive functional WB97XD with the basis set 6-31-G* in vacuo. Frequency calculation showed no negative frequencies confirming that resulting structures were in the minimum. For compounds **8d**, **9d** and **10d** the 'nosymm' input command was used. Dipole moments were obtained from the output fchk file.

ACKNOWLEDGEMENTS

This work was supported by the University Paul Sabatier (Toulouse, France) and the Centre National de la Recherche Scientifique (CNRS). It has received funding from the European Union's Horizon 2020 research and innovation program under the project MEMO, grant agreement No 766864 and from the JSPS KAKENHI grant in aid for Scientific Research on Innovative Areas "Molecular Engine (No.8006)" 18H05419. C.J.M. thanks the JSPS KAKENHI Grant-in-Aid for Early-Career Scientists (19K15312) Y.G. thanks the French Ministry of National Education for a PhD Fellowship. We would like also to thank Dr. M. Miyake and Dr. T. Shikano (Institute for Research Initiatives, NAIST) for their constant support in the management of our International Collaborative Laboratory for Supraphotocatalytic Systems between CEMES and NAIST from 2014. The DFT calculations appearing in this article were performed using HPC resources from CALMIP (Grant 2020-p20041).

KEYWORDS: molecular machines • nanocar • porphyrinoids • donor-acceptor systems • triptycene

REFERENCES

- [1] C. Kammerer, G. Erbland, Y. Gisbert, T. Nishino, K. Yasuhara, G. Rapenne, *Chem. Lett.* **2019**, *48*, 299–308.
- [2] G. Jimenez-Bueno, G. Rapenne, *Tetrahedron Lett.* **2003**, *44*, 6261–6263.
- [3] Y. Shirai, A. J. Osgood, Y. Zhao, K. F. Kelly, J. M. Tour, *Nano Lett.* **2005**, *5*, 2330–2334.
- [4] H.-P. Jacquot de Rouville, R. Garbage, F. Ample, A. Nickel, J. Meyer, F. Moresco, C. Joachim, G. Rapenne, *Chem. Eur. J.* **2012**, *18*, 8925–8928.
- [5] T. Kudernac, N. Ruangsapapichat, M. Parschau, B. Macia, N. Katsonis, S. R. Harutyunyan, K.-H. Ernst, B. L. Feringa, *Nature* **2011**, *479*, 208–211.
- [6] C. Joachim, G. Rapenne, *ACS Nano* **2013**, *7*, 11–14.
- [7] G. Rapenne, C. Joachim, *Nat. Rev. Mat.* **2017**, *2*, 17040.
- [8] R. Pawlak, T. Meier, N. Renaud, M. Kisiel, A. Hinaut, T. Glatzel, D. Sordes, C. Durand, W.-H. Soe, A. Baratoff, C. Joachim, C. E. Housecroft, E. C. Constable, E. Meyer, *ACS Nano* **2017**, *11*, 9930–9940.
- [9] M. Raeisi, K. Kotturi, K. Perumal, R. Rabbani, S.-W. Hla, E. Masson, *Abstr. Pap. Am. Chem. Soc.* **2017**, *254*, 540.
- [10] G. J. Simpson, V. García-López, P. Petermeier, L. Grill, J. M. Tour, *Nature Nanotechnol.* **2017**, *12*, 604–606.
- [11] H.-P. Jacquot de Rouville, C. Kammerer, G. Rapenne, *Molecules* **2018**, *23*, 612–623.
- [12] W.-H Soe, Y. Shirai, C. Durand, Y. Yonamine, K. Minami, X. Bouju, M. Kolmer, K. Ariga, C. Joachim, W. Nakanishi, *ACS Nano* **2017**, *11*, 10357–10365.
- [13] F. Eisenhut, C. Durand, F. Moresco, J.-P. Launay, C. Joachim, *Eur. Phys. J. Appl. Phys.* **2016**, *76*, 10001.

- [14] R. Pawlak, T. Meier, *Nature Nanotechnol.* **2017**, *12*, 712.
- [15] H.-P. Jacquot de Rouville, R. Garbage, R. E. Cook, A. R. Pujol, A. M. Sirven, G. Rapenne, *Chem. Eur. J.* **2012**, *18*, 3023–3031.
- [16] *Iptycenes chemistry from synthesis to applications*, ed. by C. F. Chen, Y. X. Ma, Springer-Verlag, Berlin, **2013**.
- [17] W.-H. Soe, C. Durand, S. Gauthier, H.-P. Jacquot de Rouville, C. Kammerer, G. Rapenne, C. Joachim, *Nanotechnology* **2018**, *29*, 495401.
- [18] G. Vives, H.-P. Jacquot de Rouville, A. Carella, J.-P. Launay, G. Rapenne, *Chem. Soc. Rev.* **2009**, *38*, 1551–1561.
- [19] U.G.E. Perera, F. Ample, H. Kersell, Y. Zhang, G. Vives, J. Echeverria, M. Grisolia, G. Rapenne, C. Joachim, S.-W. Hla, *Nature Nanotechnol.* **2013**, *8*, 46–51.
- [20] Y. Zhang, H. Kersell, R. Stefak, J. Echeverria, V. Iancu, U. G. E. Perera, Y. Li, A. Deshpande, K.-F. Braun, C. Joachim, G. Rapenne, S.-W. Hla, *Nature Nanotechnol.* **2016**, *11*, 706–712.
- [21] T. Sasaki, J. M. Tour, *Tetrahedron Lett.* **2007**, *48*, 5821–5824.
- [22] The second Nanocar Race could be postponed due to the COVID-19 sanitary crisis.
- [23] F. Chevalier, G. R. Geier, J. S. Lindsey, *J. Porphyr. Phthalocyanines* **2002**, *6*, 186–197.
- [24] G. Hu, H. S. Kang, A. K. Mandal, A. Roy, C. Kirmaier, D. F. Bocian, D. Holten, J. S. Lindsey, *RSC Adv.* **2018**, *8*, 23854–23874.
- [25] L. Grill, K.-H. Rieder, F. Moresco, G. Jimenez-Bueno, C. Wang, G. Rapenne, C. Joachim, *Surf. Science* **2005**, *584*, 153–158.
- [26] L. Grill, K.-H. Rieder, F. Moresco, G. Rapenne, S. Stojkovic, X. Bouju, C. Joachim, *Nature Nanotechnol.* **2007**, *2*, 95–98.
- [27] P. S. Bols, H. L. Anderson, *Acc. Chem. Res.* **2018**, *51*, 2083–2092.
- [28] M.J. Frisch et al. (see SI for full author list) Gaussian 09 Revision A.02, Gaussian Inc. Wallingford CT, **2009**.
- [29] A. Verykios, M. Papadakis, A. Soultati, M.-C. Skoulikidou, G. Papaioannou, S. Gardelis, I. D. Petsalakis, G. Theodorakopoulos, V. Petropoulos, L. C. Palilis, M. Fakis, N. A. Vainos, D. Alexandropoulos, D. Davazoglou, G. Pistolis, P. Argitis, A. G. Coutsolelos, M. Vasilopoulou, *ACS Omega* **2018**, *3*, 10008–10018.
- [30] G. R. Geier III, J. S. Lindsey, *Tetrahedron* **2004**, *60*, 11435–11444.
- [31] G. Rapenne, G. Jimenez-Bueno, *Tetrahedron* **2007**, *63*, 7018–7026.
- [32] S. L. Darling, E. Stulz, N. Feeder, N. Bampos, J. K. M. Sanders, *New J. Chem.* **2000**, *24*, 261–264.
- [33] (a) C. M. Cardona, W. Li, A. E. Kaifer, D. Stockdale, G. C. Bazan, *Adv. Mater.* **2011**, *23*, 2367–2371; (b) J.-C. Chambron, C. O. Dietrich-Buchecker, G. Rapenne, J.-P. Sauvage, *Chirality* **1998**, *10*, 125–133.
- [34] S. Mathew, A. Yella, P. Gao, R. Humphry-Baker, B. F. E. Curchod, N. Ashari-Astani, I. Tavernelli, U. Rothlisberger, M. Nazeeruddin, M. Grätzel, *Nat. Chem.* **2014**, *6*, 242–247.
- [35] L.-L. Li, E. W.-G. Diau, *Chem. Soc. Rev.* **2013**, *42*, 291–304.
- [36] M.-L. Seol, S.-J. Choi, C.-H. Kim, D.-I. Moon, Y.-K. Choi, *ACS Nano* **2012**, *6*, 183–189.
- [37] M. Calik, F. Auras, L. M. Salonen, K. Bader, I. Grill, M. Handloser, D. D. Medina, M. Dogru, F. Löbermann, D. Trauner, A. Hartschuh, T. Bein, *J. Am. Chem. Soc.* **2014**, *136*, 17802–17807.
- [38] F. Li, N. Gao, H. Xu, W. Liu, H. Shang, W. Yang, M. Zhang, *Chem. Eur. J.* **2014**, *20*, 9991–9997.
- [39] B. Donnio, D. W. Bruce, *J. Chem. Soc., Dalton Trans.* **1997**, 2745–2756.
- [40] Bruker, SADABS, Bruker AXS Inc., Madison, Wisconsin, USA, **2008**.
- [41] ShelXT, G. M. Sheldrick, University of Göttingen, *Acta Crystallogr. Sect. A*, **2015**, *71*, 3–8.
- [42] A. L. Spek, A. L. *Acta Crystallogr. Sect. C*, **2015**, *71*, 9–18.